

# Dilepton production at HADES: theoretical predictions

M.D. Cozma, C. Fuchs, E. Santini, and A. Fässler  
*Institut für Theoretische Physik, Universität Tübingen,  
Auf der Morgenstelle 14, 72076 Tübingen, Germany*

Dileptons represent a unique probe for nuclear matter under extreme conditions reached in heavy-ion collisions. They allow to study meson properties, like mass and decay width, at various density and temperature regimes. Present days models allow generally a good description of dilepton spectra in ultra-relativistic heavy ion collision. For the energy regime of a few GeV/nucleon, important discrepancies between theory and experiment, known as the DLS puzzle, have been observed. Various models, including the one developed by the Tübingen group, have tried to address this problem, but have proven only partially successful. High precision spectra of dilepton emission in heavy-ion reactions at 1 and 2 GeV/nucleon will be released in the near future by the HADES Collaboration at GSI. Here we present the predictions for dilepton spectra in C+C reactions at 1 and 2 GeV/nucleon and investigate up to what degree possible scenarios for the in-medium modification of vector mesons properties are accessible by the HADES experiment.

PACS numbers: 12.40Vv,25.75.-q,25.75Dw

## I. INTRODUCTION

Heavy ion reactions present an unique opportunity for the study of nuclear matter under extreme conditions allowing a comprehensive analysis of the phase structure of the underlying theory of strong interactions. In this process electromagnetic probes such as dileptons have been proven to be most effective since they leave the reaction zone essentially undistorted by final state interactions. They provide thus a clear view on effective degrees of freedom at high baryon density and temperature. It has been argued that their differential spectra could reveal information about chiral restoration and in-medium properties of hadrons [1, 2, 3]. Theoretically, there exists an abundance of models that predict a change of vector meson masses and widths in high density/temperature nuclear matter: Brown-Rho scaling [1] is equivalent with a decrease of vector meson masses in nuclear medium; models based on QCD sum rules [2] and effective hadronic models [4, 5] reach similar conclusions.

Experimentally, dilepton spectra have been measured at two different energy regimes: the CERES [6, 7], HELIOS [8] and recently NA60 [9] at CERN have measured dielectrons and dimuons,

respectively, in heavy ion reactions at 158 GeV/nucleon. In proton-nucleus reactions the sum over all measured hadronic sources, i.e. the so-called hadronic cocktail, describes the corresponding dilepton spectra perfectly well. However, in heavy systems (Pb+Au) a significant enhancement of the dilepton spectra below the  $\rho$  and  $\omega$  peaks has been observed relative to the corresponding hadronic cocktail. Such a behaviour could be explained theoretically, within a scenario of a dropping  $\rho$  vector meson mass [10] or by the inclusion of in-medium spectral functions for the vector mesons [11, 12]. The recent NA60 dimuon spectra with high resolution in the vicinity around the  $\rho$ - $\omega$  peak seem to rule out a naive dropping mass scenario but support the picture of modified  $\rho$ - $\omega$  spectral functions. An enhanced strength below the  $\omega$  peak has also been observed in  $\gamma$ -nucleus reactions [13]. A second set of heavy ion experiments have been performed at laboratory energies of 1.0 AGeV (Ca+Ca and C+C) by the DLS Collaboration at BEVALAC [14, 15]. Also in this case, the low mass region of the dilepton spectra is underestimated by present transport calculations, in contrast with similar measurements (1.04 - 4.88 GeV/nucleon) for the p+p and p+d systems. As opposed to the ultra-relativistic case, the situation does not improve when the in-medium spectral functions or the dropping mass scenarios are taken into account [12, 16] (the DSL puzzle). Other scenarios like possible contributions from the quark-gluon plasma or in-medium modifications of the  $\eta$  mass have been excluded as a possible resolution of this puzzle. Decoherence effects [17] have been proven to be partially successful in explaining the difference between the DLS data and the theoretical predictions.

Recently, a new measurement by the HADES Collaboration at GSI has been completed and the results will be published in the near future [18]. The aim of this second generation experiment is to measure dilepton spectra in A+A, p+A and  $\pi$ +A reactions with an unprecedented mass resolution ( $\Delta M/M \simeq 1\%(\sigma)$ ) over the entire spectrum [19]. Such a resolution allows to measure the in-medium properties (mass and width) of  $\rho$  and  $\omega$  mesons through their decays into dielectron pairs in nuclear matter with high precision and will put strong constraints on theoretical models. This letter presents predictions of the dilepton production in C+C reactions at 1.0 and 2.0 AGeV which are those reactions where first data from HADES will be available in the near future. The vector meson and dilepton production is described within the framework of the resonance model developed in [20, 21, 22] in combination with the relativistic quantum molecular dynamics (RQMD) transport model for heavy ion collisions [17]. The influence of medium effects such as quantum decoherence, collisional broadening and a dropping vector meson mass are investigated. The paper is organised as follows: in Section II we give a brief description of the elementary reactions which contribute to dilepton emission in heavy ion collisions, together with an outline of the RQMD model. Section

III is devoted to the presentation of our prediction for the differential mass spectrum of dilepton production in 1.0 and 2.0 AGeV C+C collisions. We conclude with Section IV.

## II. THE MODEL

### A. Elementary dilepton sources

The elementary sources of dilepton production in heavy ion reaction in the energy range of a few GeV/nucleon are numerous. One can identify three main classes of processes that lead to dilepton emission: nucleon-nucleon bremsstrahlung, decays of light unflavoured mesons and decay of nucleon and  $\Delta$  resonances. For the energy range of interest in this paper dilepton generation through nucleon-nucleon bremsstrahlung is unimportant. Feynman diagrams of processes belonging to the last two classes are depicted in Fig. (1).

At incident energies of 1 AGeV the cross-sections for meson production  $\mathcal{M} = \eta, \eta', \rho, \omega, \phi$  are small and these mesons do not play an important role in the dynamics of heavy-ion collisions. Their production can thus be treated perturbatively, in contrast to the case of the pion. The decay to a dilepton pair takes place through the emission of a virtual photon. The differential branching ratios for the decay of a meson to a final state  $Xe^+e^-$  can be written

$$dB(\mu, M)^{\mathcal{M}, \pi \rightarrow e^+e^-X} = \frac{d\Gamma(\mu, M)^{\mathcal{M}, \pi \rightarrow e^+e^-X}}{\Gamma_{tot}^{\mathcal{M}, \pi}(\mu)}, \quad (1)$$

with  $\mu$  the meson mass and  $M$  the dilepton mass. Three types of such decays have been considered: direct decays  $\mathcal{M} \rightarrow e^+e^-$  (Fig. 1a), Dalitz decays  $\mathcal{M} \rightarrow \gamma e^+e^-$ ,  $\mathcal{M} \rightarrow \pi(\eta)e^+e^-$  (Fig. 1b) and four-body decays  $\mathcal{M} \rightarrow \pi\pi e^+e^-$  (Fig. 1c). A comprehensive study of the decay of light mesons to a dilepton pair has been performed in [20], the decay channels there are most important quantitatively for heavy-ion collisions at 1 and 2 GeV/nucleon being  $\pi^0 \rightarrow \gamma e^+e^-$  and  $\eta \rightarrow \gamma e^+e^-$ .

The third source for dilepton emission we have mentioned was the decay of baryonic resonances (see Fig. 1d). For the description of this process an extension of the vector meson dominance (VMD) model has been employed [20, 21]. The original VMD model assumes that decays of baryon resonances run through an intermediate virtual meson ( $\rho$  or  $\omega$ ) required for the description of the form-factors entering in the calculation of the radiative ( $R \rightarrow N\gamma$ ) and mesonic ( $R \rightarrow NV$ ) decays. Such a model does not allow the simultaneous description of both radiative and mesonic decays [5, 22, 23]. Furthermore the quark counting rules require a stronger suppression of the transition form-factor than the  $1/t$  behaviour predicted by the naive VMD. Similarly the  $\omega\pi\gamma$  transition form-factor shows an asymptotic  $1/t^2$  behaviour [24]. An extension of the VMD to allow

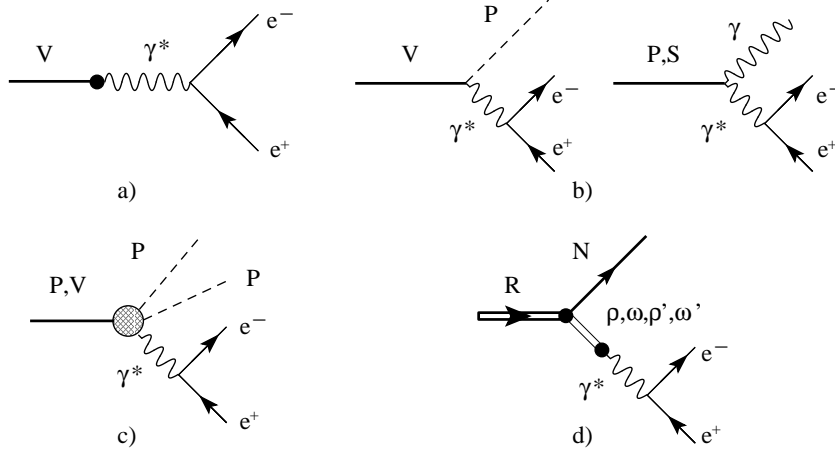


FIG. 1: Feynman diagrams of the elementary processes contributing to dilepton emission: a) direct decay of a vector meson ( $\rho, \omega, \phi$ ) to a dilepton pair going through an intermediate photon (VMD model); b) Dalitz decays of a vector (V), pseudo-scalar (P) or scalar meson (S) into a dilepton pair and a photon or a pseudo-scalar meson ( $\eta$  or  $\pi$ ); c) four-body decay into a dilepton pair plus two pseudo-scalar mesons (the hashed vertex represents an intermediate state containing a vector mesons and/or virtual photon - see Ref. [20]); and d) the decay of a nucleon or  $\Delta$  resonance into a nucleon plus a virtual vector meson (extended VMD) which then decays into two dileptons.

contributions from radially excited vector mesons ( $\rho(1250), \rho(1450), \dots$  in Ref. [21]) that interfere destructively with the ground state vector mesons ( $\rho$  in this example) allow for a resolution of the mentioned problems of the original VMD and describe the radiative and mesonic decays in a unitary way.

In terms of the branching ratios for the Dalitz decays of the baryon resonances, the cross section for  $e^+e^-$  production from the initial state  $X'$  together with the final state  $NX$  can be written

$$\frac{d\sigma(s, M)^{X' \rightarrow NX e^+ e^-}}{dM^2} = \sum_R \int_{(m_N + M)^2}^{\sqrt{s} - m_X} d\mu^2 \quad (2)$$

$$\times \frac{d\sigma(s, \mu)^{X' \rightarrow RX}}{d\mu^2} \sum_V \frac{dB(\mu, M)^{R \rightarrow VN \rightarrow Ne^+ e^-}}{dM^2},$$

where  $\mu$  is the mass of the baryon resonance  $R$  which has the production cross-section  $d\sigma(s, \mu)^{X' \rightarrow XR}$  and  $dB(\mu, M)^{R \rightarrow VN \rightarrow Ne^+ e^-}$  being the differential branching ratio for the decay of the resonance  $R \rightarrow Ne^+e^-$  through the vector meson  $V$ . The initial state  $X'$  could consist of two baryons ( $X' = NN, NR, RR'$ ) or of one nucleon and a pion ( $X = \pi N$ ). The dilepton decay rate can be found, once the width  $\Gamma(R \rightarrow N\gamma^*)$  is known by using the factorisation prescription

$$d\Gamma(R \rightarrow Ne^+e^-) = \Gamma(R \rightarrow N\gamma^*) M \Gamma(\gamma^* \rightarrow e^+e^-) \frac{dM^2}{\pi M^4}, \quad (3)$$

with

$$M\Gamma(\gamma^* \rightarrow e^+e^-) = \frac{\alpha}{3}(M^2 + 2m_e^2)\sqrt{1 - \frac{4m_e^2}{M^2}}. \quad (4)$$

The decay width  $\Gamma(R \rightarrow N\gamma^*)$  is described within the extended VMD model [21] in terms of three transition form-factors (magnetic, electric and Coulomb) in case of a resonance with spin  $J > 1/2$  and two for  $J = 1/2$ , which is just the number of independent helicity amplitudes for the respective spin value. The free parameters of the model are fixed by constraining the asymptotic form of the form-factors by quark counting rules [25] and fitting to the experimental data for photo-production and electro-production amplitudes and partial-wave analysis for multichannel  $\pi N$  scattering. The number of intermediate  $\rho$  or  $\omega$  states required to describe the transition form-factors depends on the spin  $J$  of the resonance in question: namely  $J - 1/2 + 3$ . For the case that  $J_{max} = 7/2$  one needs 6 intermediate mesons, with the masses chosen as follows: 0.769, 1.250, 1.450, 1.720, 2.150 and 2.350 (in GeV). Within this model a consistent description of radiative and mesonic decays could be achieved. Further details about the extended VMD can be found in Ref. [21].

As already mentioned the decay widths  $\Gamma(R \rightarrow N\gamma^*)$  are expressed in terms of the magnetic, electric and Coulomb form-factors, more precisely they depend on the modulus squared of these form-factors. In the extended VMD each of these form-factors is in turn expressed as a linear superposition of the contributions from the intermediate vector mesons ( $\rho$  or  $\omega$ ):

$$G_T^{(\pm)}(M^2) = \sum_k \mathcal{M}_{Tk}^{(\pm)} \quad (5)$$

with  $T$  standing for each of possible form-factors,  $(\pm)$  denotes states of normal and abnormal parity respectively and the sum is over the intermediate mesons. The amplitude

$$\mathcal{M}_{Tk}^{(\pm)} = h_{Tk}^{(\pm)} \frac{m_k^2}{m_k^2 - im_k\Gamma_k - M^2} \quad (6)$$

represents the contribution of the  $k^{th}$  vector meson to the amplitude of type  $T$ . The residues  $h_{Tk}^{(\pm)}$  are fixed by the requirement that the asymptotic expression of the form-factors is consistent with the quark counting rules [25]. This leads to a destructive interference between the intermediate vector mesons, since quark counting rules predict a behaviour steeper for the form-factors than the  $1/M^2$  contribution of a single meson. In the medium it is expected that the coherence between the contributions of individual mesons is at least partially lost. In the extreme case of total decoherence, this would lead to the following replacement in the expression for the decay width,

$$\left| \sum_k \mathcal{M}_{Tk}^{(\pm)} \right|^2 \longrightarrow \sum_k \left| \mathcal{M}_{Tk}^{(\pm)} \right|^2, \quad (7)$$

which will result in an enhancement of the resonance contributions. In reality both, the density and wavelength of the meson are finite. Introducing the decay length  $L_D$  of a resonance and its collision length  $L_C$  one can determine the probability of coherent decay (*i.e.* the meson decay takes place before the first collision) as  $w = \frac{L_C}{L_C + L_D}$ . In order to account for the decoherence effect, one can introduce an enhancement factor  $E_T(M^2, \vec{Q}^2)$ ,

$$|G_T^{(\pm)}(M^2)|^2 \longrightarrow E_T^{(\pm)}(M^2, \vec{Q}^2) |G_T^{(\pm)}(M^2)|^2, \quad (8)$$

The dependence on the space-like part  $\vec{Q}$  of the vector meson momentum originates from the definition of the collision length  $L_C$ . Further details can be found in Ref. [17].

## B. The RQMD model

The heavy-ion reaction dynamics is described within the framework of relativistic quantum molecular dynamics. The Tübingen (R)QMD transport code [26] has been extended to include all nuclear resonances with masses below 2 GeV, in total 11  $N^*$  and 10  $\Delta$  resonances. A full list with the corresponding masses and decay widths to various channels can be found in Tables III and IV of Ref. [17]. For the description of dilepton production through baryonic resonances, respectively, the  $\rho$  and  $\omega$  production in  $NN$  and  $\pi N$  reactions, only the well established ( $4^*$ ) resonances listed by PDG [27] are taken into account. This corresponds to the same set of resonances which has been used for the description of vector meson and dilepton production in elementary (p+p) reactions [22, 28], see also [17, 29]. As necessary for the present investigations, it provides e.g. an accurate reproduction of the measured pion yields in C+C reactions [30] within error bars. For the case of the  $\eta$  meson, the fit of Ref. [31] is used and therefore the production through the decay of nucleonic resonances is completely neglected. A check of the two production mechanisms  $NN \rightarrow NN\eta$  and  $NN \rightarrow RN \rightarrow NN\eta$  has been performed leading to an almost similar  $\eta$  yield in heavy ion reactions.  $\eta$  absorption runs over the  $N^*(1535)$  resonance. The corresponding  $\eta$  production cross sections in C+C collisions are consistent with the experimental results of Ref. [32].

## III. PREDICTIONS FOR HADES

It is expected that in nuclear matter the  $\rho$  and  $\omega$  mesons change their properties. Estimates for the collisional broadening of  $\rho$  in hadronic matter (nuclear matter or pionic gas) predict a collisional width of the order of the vacuum width. For the  $\omega$  the vacuum width is only 8.4 MeV whereas in medium is expected to be more than one order of magnitude larger. The dilepton

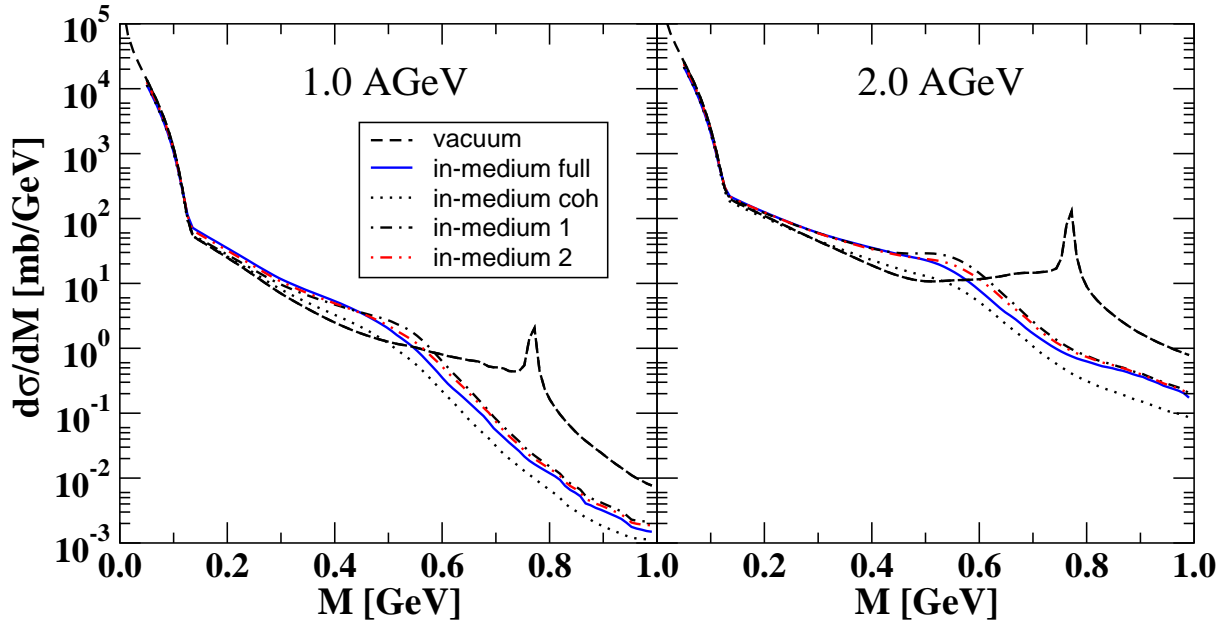


FIG. 2: Dilepton spectrum in C+C at 1 AGeV (left panel) and 2 AGeV (right panel). Besides the vacuum calculation (dashed line) four different scenarios for in-medium modifications of the dilepton yield are presented. The full in-medium calculation (full line) takes into account Brown-Rho scaling for the vector meson masses, collisional broadening ( $\Gamma_\rho^{\text{tot}}=250$  MeV,  $\Gamma_\omega^{\text{tot}}=125$  MeV) and decoherence effects. The three other in-medium calculations differ from the full one in the following respects:  $\Gamma_\rho^{\text{tot}}=150$  MeV (vacuum value) for the dashed-dotted curve, no decoherence effects for the dotted curve, and  $\Gamma_\rho^{\text{tot}}=200$  MeV together with  $\Gamma_\omega^{\text{tot}}=60$  MeV (double-dot-dashed curve).

spectra at intermediate energies, like those probed by the HADES and also the DLS experiments, are more sensitive to the  $\omega$  meson collisional broadening. In absence of such modifications the invariant mass dilepton spectrum would show a pronounced  $\omega$  peak. In the DLS experiment such an enhancement has not been observed. Despite the limited mass resolution in [17] an in-medium  $\omega$  width of  $\Gamma_\omega^{\text{tot}} = 100 \div 300$  MeV at nuclear matter density  $\rho = 1.5\rho_0$  has been extracted from the DLS data. The modification of the  $\rho$  width was found to be similar in magnitude, i.e.  $\Gamma_\rho^{\text{tot}} = 200 \div 300$  MeV (again at  $\rho = 1.5\rho_0$ ). In the present calculations a linear density dependence of the  $\rho$  and  $\omega$  decay widths is assumed, i.e.  $\Gamma_V^{\text{tot}} = \Gamma_V^{\text{vac}} + \rho/\rho_0 \Gamma_V^{\text{coll}}$ . As an additional in-medium effect the masses of the mesons are supposed to vary as a function of the nuclear matter density at the point where the resonance decay occurs, following a Brown-Rho scaling law  $m_V^* = m_V(1 - \alpha\rho/\rho_0)$  with  $\rho$  the local baryon density and  $\alpha = 0.2$ . In contrast to [17] the dropping mass scenario is now included in addition to the collisional broadening and decoherence medium effects.

A second medium effect is the due to decoherence, which mostly affects the dilepton spectrum

below the  $\rho/\omega$  peak. The probability for coherent decay depends both on the in-vacuum decay widths (through  $L_D$ ) and the collisional broadening (through  $L_C$ ). For the ground state vector mesons the following values for the collisional widths have been adopted:  $\Gamma_\rho^{\text{coll}}=100$  MeV and  $\Gamma_\omega^{\text{coll}}=116.6$  MeV at  $\rho = \rho_0$  with the same values for their radially excited states that enter in the built up of the extended VMD. The vacuum widths of the radially excited mesons are larger than those of the ground state  $\rho$  and  $\omega$  meson and as a consequence they tend to decay coherently. The decoherence effect is largest for the  $\omega$  vector meson since its vacuum width is very small.

The results for C+C collisions at 1 and 2 AGeV are shown in Fig. (2). Besides the dilepton spectrum with in-vacuum properties of the intermediate mesons (depicted by a dashed line) the effects of three different in-medium scenarios on the same spectrum are also shown. The calculation in which all the in-medium effects are included to their full extent is depicted by a full line. This case corresponds to maximal collisional broadening, i.e.  $\Gamma_\omega^{\text{tot}}=125$  MeV,  $\Gamma_\rho^{\text{tot}}=250$  MeV, both at  $\rho = \rho_0$ , and it includes Brown-Rho scaling for the meson masses and decoherence effects.

The remaining three calculations provide insight on the significance of the individual in-medium effects, even though strictly speaking they cannot be disentangled. The variation of the  $\rho$  meson width between  $\Gamma_\rho^{\text{tot}} = 150 \div 250$  MeV leads to a modification of the dilepton yield by a factor of 2 in the dilepton mass range 0.5-0.8 GeV (compare the full and dashed-dotted curves). Decoherence effects in nuclear medium are responsible for at most a 50% change in the dilepton spectra at intermediate masses (dotted and full lines).

Some of the  $\omega$  mesons, produced in the final stages of the collision or at the surface of the interaction region might escape with vacuum properties and therefore lead to a small peak in the dilepton cross-section. The density dependent meson widths include these possibilities. To explore the possibility of a reminiscent  $\omega$  peak in more detail an additional calculation with a moderate in-medium  $\omega$  width  $\Gamma_\omega^{\text{tot}}= 60$  MeV, together with  $\Gamma_\rho^{\text{tot}}=200$  MeV, (again at  $\rho_0$ ) is shown. It should be noted that such a value for  $\Gamma_\omega^{\text{tot}}$  is in agreement with the analysis of [13] from photo-nucleus reactions. An increase of at most 50% in the dilepton yield is observed with respect to the full 'in-medium' scenario in the 0.4-0.8 GeV mass region, with no sign of a sharp peak.

The effect of the Brown-Rho scaling is well known: it produces a shift of the  $\rho/\omega$  peak from its vacuum position towards lower dilepton invariant masses, namely around 0.6 GeV. The peak dissolves once the width of the  $\omega$  meson is changed to its in-medium value. All results have been obtained with a strong  $N^*(1535)N\omega$  coupling as enforced by the fit of the resonance model parameter to nucleon resonance electro- and photo-production [21] and which has been used in



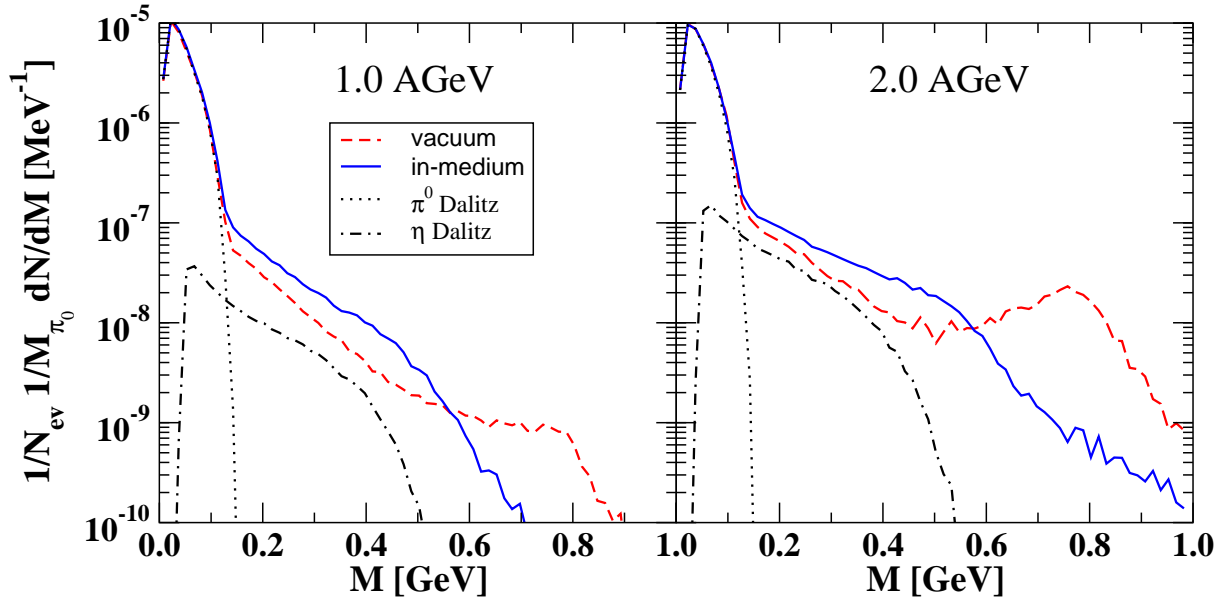


FIG. 3: Dilepton spectrum in C+C reactions at 1.0 and 2.0 AGeV after application of the full HADES acceptance filter. Calculations without (vacuum) and including in-medium effects (in-medium), i.e. maximal  $\rho$  and  $\omega$  collisional broadening, mass shifts and decoherence, are shown.

[17, 28].

The results of Fig. (2) are pure theoretical results, *i.e.* they have not been filtered in order to account for the experimental detector acceptance. Such a procedure is, however, indispensable for a meaningful comparison to data. In order to investigate up to what degree the HADES experiment will be able to discriminate between the different scenarios, we apply in the following the full HADES acceptance filter in combination with a smearing procedure for the corresponding HADES mass resolution. The filtered results are shown in in Fig. 3. The 'in-medium' calculation contains the combination of all medium effects under consideration, i.e.  $\rho$  and  $\omega$  collisional broadening and mass shifts and decoherence (corresponding to the full lines in Fig. (2)). The spectra are normalised to the number of events  $N_{\text{ev}}$  and to the  $\pi^0$  multiplicity. Contributions from  $\pi^0$  and  $\eta$  Dalitz decay are shown separately. The difference between the 'vacuum' and the 'in-medium' calculation is still clearly visible: most pronounced are the medium effects in the mass region around the  $\rho/\omega$  peak ( $M \sim 0.6 \div 1$  GeV) where a complete dissolution of the  $\rho$  and in particular the  $\omega$  peak is predicted. This effect is even more pronounced at 2 AGeV and the HADES experiment will be able to clearly discriminate between the 'vacuum' and the 'in-medium' scenarios.

In the low and intermediate mass region the medium effects are less pronounced, i.e. of the order of about 50%. Decoherence affects the dilepton pairs over almost the entire spectrum. It

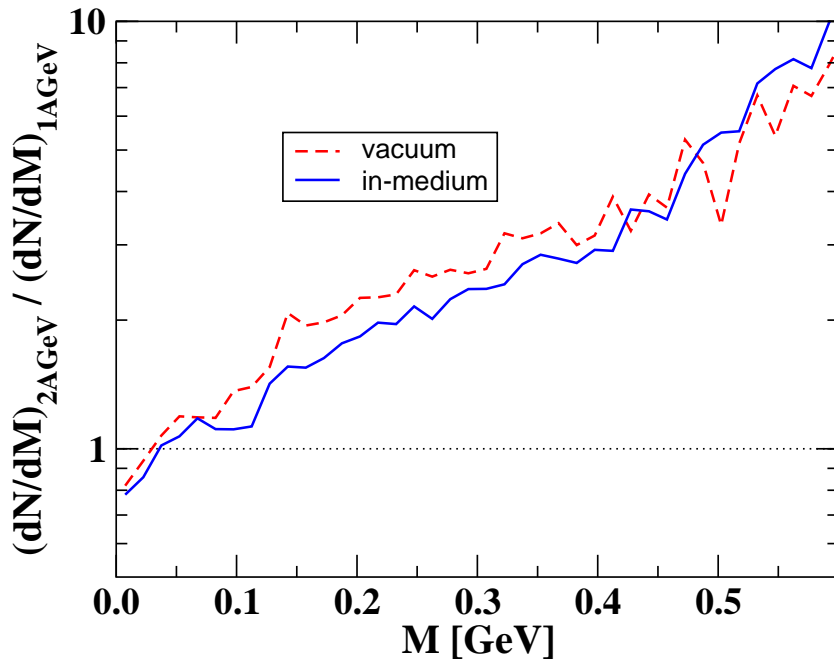


FIG. 4: Ratio of the dilepton spectrum in C+C reactions at 2.0 over 1.0 AGeV after application of the full HADES acceptance filter. Calculations without (vacuum) and including in-medium effects (in-medium), i.e.  $\rho$  and  $\omega$  collisional broadening and mass shifts and decoherence, are shown.

is, however, the only source for 'in-medium' changes at low invariant dilepton masses, below 0.4 GeV. To discriminate the various scenarios experimentally in the low and intermediate mass region will be difficult, at least in the light C+C system. However, keeping in mind that medium effects are often better visible at subthreshold energies as known e.g. from kaon production [29], it is natural to build the ratio between the spectra at 1 and 2 AGeV. This is done in Fig. (4) where the ratio of the dilepton spectra at 1 and 2 AGeV for the 'in-vacuum' (dashed line) and 'in-medium' (full line) scenarios are plotted. Here aswell the theoretical predictions have been filtered using the HADES acceptance filter which allows to infer the correctness of the conjecture concerning the relevance of such effects directly from experiment. From Fig. (4) one observes a stronger in-medium enhancement of the low mass yield at 1 AGeV compared to 2 AGeV which results in a smaller value for the ratio. The effect is, however at the 20-30% level which requires very high resolution data.

#### IV. FINAL CONCLUSIONS

In this paper we have presented predictions for the dilepton emission in heavy ion reactions at C+C at 1 and 2 AGeV. Experimental data for these two reactions will be available in the near future from the HADES collaboration at GSI. A clear distinction between 'vacuum' and 'in-

medium' scenarios for  $\rho$  and  $\omega$  properties is possible in the mass region around the  $\rho/\omega$  peak. In particular at 2 GeV the effect from an in-medium broadening of the vector mesons is dramatic and leads to a strong suppression of the spectrum. At low invariant masses the in-medium effects, in particular the decoherence, are less pronounced, i.e. on the 20-30% level, but can be expected to be more clearly seen in larger systems than C+C.

We would like to acknowledge the help of our experimental colleagues from HADES who have filtered the results of our model with the HADES filter.

- 
- [1] G.E. Brown and M. Rho, Phys. Rev. Lett. **66**, 2720 (1991); Phys. Rep. **269**, 333 (1996).
  - [2] T. Hatsuda and S.H. Lee, Phys. Rev. C **46**, R34 (1992); I. Koike, *ibid.* **51**, 1488 (1995); T. Hatsuda, S.H. Lee, and H. Shiomi, *ibid.* **52**, 3364 (1992); S. Leupold, *ibid.* **64**, 015202 (2001); S. Zschoke, O.P.Pavlenko, and B. Kämpfer, Eur. Phys. J. A **15**, 529 (2002).
  - [3] C.M. Shakin and W.D. Sun, Phys. Rev. C **49**, 1185 (1994); M. Asakawa and C.M. Rho, Phys. Rev. C **48**, R526 (1993); N. Kaiser and W. Weise, Nucl. Phys. A **624**, 527 (1997).
  - [4] M. Hermann, B. Friman, and W. Nörenberg, Nucl. Phys. A **560**, 411 (1993); G. Chanfray and P. Schuck, Nucl. Phys. A **545**, 271c (1992); R. Rapp, G. Chanfray, and J. Wambach, Nucl. Phys. A **617**, 472 (1997).
  - [5] B. Friman and H.J. Pirner, Nucl. Phys. A **617**, 496 (1997).
  - [6] G. Agakichiev *et al.* [CERES Collaboration], Phys. Rev. Lett. **75**, 1272 (1995).
  - [7] A. Marin, *et al.* [CERES Collaboration], J. Phys. G30 (2004) S709.
  - [8] M.A. Mazzoni, Nucl. Phys. A **566**, 95c (1994); M. Masera, Nucl. Phys. A **590**, 93c (1995).
  - [9] R. Arnaldi *et al.* [NA60 Collaboration], Phys. Rev. Lett. **96** (2006) 162302.
  - [10] W. Cassing, W. Ehehalt, and C.M. Ko, Phys. Lett. B **363**, 35 (1995); G.Q. Li, C.M. Ko, and G.E. Brown, Nucl. Phys. A **606**, 568 (1996); C.M. Hung and E.V. Shuryak, Phys. Rev. C **56**, 453 (1997).
  - [11] M. Urban, M. Buballa, R. Rapp, and J. Wambach, Nucl. Phys. A **641**, 433 (1998); Nucl. Phys. A **673**, 357 (2000); R. Rapp and J. Wambach, Adv. Nucl. Phys. **25**, 1 (2000);
  - [12] E.L. Bratkovskaya, W. Cassing, R. Rapp, and J. Wambach, Nucl. Phys. A **634**, 168 (1998).
  - [13] D. Trnka *et al.* [CBELSA/TAPS Collaboration], Phys. Rev. Lett. **94** (2005) 192303
  - [14] R.J. Porter *et al.* [DLS Collaboration], Phys. Rev. Lett. **79**, 1229 (1997).
  - [15] W.K. Wilson *et al.* [DLS Collaboration], Phys. Rev. **C57** (1998) 1865.
  - [16] C. Ernst, S.A. Bass, M. Belkacem, H. Stocker, and W. Greiner, Phys. Rev. C **58**, 447 (1998); E.L. Bratkovskaya and C.M. Ko, Phys. Lett. B **445**, 265 (1999).
  - [17] K. Shekter, C. Fuchs, A. Faessler, M. Krivoruchenko, and B. Martemyanov, Phys. Rev. C **68**, 014904 (2003).
  - [18] HADES Collaboration, private communication.

- [19] J. Friese, HADES Collaboration, *Prog. Part. Nucl. Phys.* **42**, 235 (1999).
- [20] A. Faessler, C. Fuchs, and M.I. Krivoruchenko, *Phys. Rev. C* **61**, 035206 (2000).
- [21] M.I. Krivoruchenko, B.V. Martemyanov, A. Faessler, and C. Fuchs, *Ann. Phys.* **296**,
- [22] A. Faessler, C. Fuchs, M.I. Krivoruchenko, and B.V. Martemyanov, *J. Phys. G* **29**, 603 (2003).
- [23] M. Post and U. Mosel, *Nucl. Phys. A* **688**, 808 (2001).
- [24] A.I. Vainstein and V.I. Zakharov, *Phys. Lett. B* **72**, 368 (1978).
- [25] S.J. Brodsky and G.R. Farrar, *Phys. Rev. Lett.* **31**, 1153 (1973); S.J. Brodsky and G.R. Farrar, *Phys. Rev. C* **11**, 1309 (1975).
- [26] W.S. Uma Maheswari, C. Fuchs, A. Faessler, L. Sehn, D. Kosov, and Z. Wang, *Nucl. Phys. A* **628**, 669 (1998).
- [27] Particle Data Group, *Phys. Rev. D* **54**, 1 (1996).
- [28] C. Fuchs, M.I. Krivoruchenko, H. Yadav, A. Faessler, B.V. Martemyanov, and K. Shekther, *Phys. Rev. C* **67**, 025202 (2002).
- [29] C. Fuchs, *Prog. Part. Nucl. Phys.* **56** (2006) 1.
- [30] C. Sturm et al. [KaoS Collaboration], *Phys. Rev. Lett.* **86** (2001) 39.
- [31] A. Sibirtsev, W. Cassing, and U. Mosel, *Z. Phys. A* **358**, 357 (1997).
- [32] R. Averbek, R. Holzmann, V. Metag, and R.S. Simon, *Phys. Rev. C* **67**, 024903 (2003).